Inorg. Chem. **2005**, *44*, 666–672

Aerobic Oxidation of Formaldehyde Mediated by a Ce-Containing Polyoxometalate under Mild Conditions

Oxana A. Kholdeeva,*,† Maria N. Timofeeva,† Gennadii M. Maksimov,† Raisa I. Maksimovskaya,† Wade A. Neiwert,‡ and Craig L. Hill*,‡

Boreskov Institute of Catalysis, Pr. Lavrentieva 5, Novosibirsk 630090, Russia, and Department of Chemistry, Emory University, 1515 Pierce Drive, Atlanta, Georgia 30322

Received July 7, 2004

An evaluation of over 50 polyoxometalates (POMs) identified the complex $NaH_3[SiW_{11}Ce^{IV}O_{39}]$ (**$NaH_3$1**) as a selective and effective catalyst for the aerobic oxidation of formaldehyde to formic acid under very mild (including ambient) conditions. ^{183}W NMR, UV–vis, cyclic voltammetry, and potentiometric titration establish that the catalyst is a monomer (C_s symmetry), **1**, in solution, while X-ray crystallography ($a = 12.9455(15)$ Å, $b = 13.2257(16)$ Å, $c = 14.5288(17)$ Å, $\alpha = 81.408(2)°$, $\beta = 85.618(2)°$, $\gamma = 80.726(2)°$, $P\bar{1}$, $Z = 1$, R1 = 5.79% based on 17244 independent reflections) and IR establish it to be a dimer (C_i symmetry), **1_2**, in the solid state. Several lines of evidence, including the parabolic kinetic order in **1**, nonlinear Arrhenius plot, independence of the rate on O_2 pressure, presence of titratable H_2O_2 and HCO_3H intermediates, and inhibition by conventional radical scavengers, all indicate the O_2-based oxidations proceed by complex homolytic chemistry (autoxidation and Haber–Weiss radical-chain processes) likely initiated by protonated **1**.

Introduction

The development of catalysts for the oxidation of organic compounds by air (O_2) under ambient conditions is of both academic and practical importance.[1−4] High on the list of target molecules for aerobic oxidation under ambient conditions is formaldehyde. Formaldehyde is a suspect carcinogen that is fairly ubiquitous in indoor air and a cause of "sick building syndrome". It outgasses from building materials, fillers, and coatings.[5,6] As a consequence, developing materials that catalyze its oxidation by the air itself (O_2) to the far less toxic formic acid, eq 1, and/or CO and CO_2, which are readily removed by ventilation, would be very attractive.

$$CH_2O + {}^1/_2O_2 \rightarrow HCOOH \qquad (1)$$

However, this process is quite challenging because formaldehyde is far harder to oxidize, either by autoxidation (radical-chain reductant-free O_2-based oxidation) or by other oxidation processes, than nearly all aldehydes and ketones. Catalysis of eq 1 has been thoroughly studied and is well-known at high temperature ($T > 120$ °C),[7,8] but it has yet to be achieved under ambient conditions (using simply room air). The difficulty in oxidizing formaldehyde derives in part from the fact that it exists in hydrated or otherwise complexed forms in human environments; the reactive keto form is present only in miniscule concentrations. Water is ubiquitous in these environments, and the hydration equilibrium for formaldehyde, eq 2, unlike that of nearly all aldehydes and ketones, lies far to the right ($K \sim 10^4$ at 20 °C).[9]

$$CH_2O + H_2O \overset{K_{eq}}{\rightleftharpoons} CH_2(OH)_2 \qquad (2)$$

Transition-metal−oxygen-anion clusters (polyoxometalates or POMs for short) due to their unique properties, including

* To whom correspondence should be addressed. E-mail: khold@catalysis.nsk.su (O.A.K.); chill@emory.edu (C.L.H.) Fax: (+7)3832-34-30-56 (O.A.K.); 404-727-6076 (C.L.H.).
† Boreskov Institute of Catalysis.
‡ Emory University.

(1) Brink, G.-J.; Arends, I. W. C. E.; Sheldon, R. A. *Science* **2000**, *287*, 1636−1639.
(2) Xu, L.; Boring, E.; Hill, C. L. *J. Catal.* **2000**, *195*, 394−405.
(3) Boring, E.; Geletii, Y. V.; Hill, C. L. *J. Am. Chem. Soc.* **2001**, *123*, 1625−1635.
(4) Rhule, J. T.; Neiwert, W. A.; Hardcastle, K. I.; Do, B. T.; Hill, C. L. *J. Am. Chem. Soc.* **2001**, *123*, 12101−12102.
(5) Harrison, R. M. In *Indoor Air Pollution and Haelth*; Hester, R. E., Harrison, R. M., Eds.; Royal Society of Chemistry: Cambridge, 1996; Vol. 10, pp 101−126.
(6) Kelly, T. J.; Smith, D. L.; Satola, J. *Environ. Sci. Technol.* **1999**, *33*, 81−88.
(7) Ai, M. *J. Catal.* **1983**, *83*, 141−150.
(8) Popova, G. Y.; Andrushkevich, T. V. *Kinet. Catal. (Engl Transl.)* **1997**, *38*, 258−261.
(9) Bieber, R.; Trumpler, G. *Helv. Chim. Acta* **1947**, *30*, 1860−1865.

10.1021/ic049109o CCC: $30.25
Published on Web 01/13/2005

metal-oxide-like structure, thermal and hydrolytic stability, tunability of acid and redox properties, solubility in various media, etc., are attractive oxidation catalysts.[10−17] Moreover, they can be deposited on fabrics and porous materials to render these materials catalytically decontaminating.[2,18,19] Evaluation of each entry of a targeted library of complexes (50 POMs, or POM + cocatalyst combinations known or likely to catalyze oxidations; see Table S1 in the Supporting Information, SI) identified the Ce(IV)-monosubstituted polyoxometalate, $NaH_3[SiW_{11}CeO_{39}]$ (**$NaH_3$1**), that dimerizes (or polymerizes)[20,21] in the solid-state to $[(SiW_{11}CeO_{39})_2]^{8-}$ (**1_2**), as a promising catalyst for eq 1. We report here characterization of **1** and **1_2** and catalysis of eq 1 by the monomer under very mild conditions (20−60 °C and 1 atm of air or O_2).

Experimental Section

Materials. The formaldehyde solutions were prepared by diluting 35.5% aqueous formalin, containing 2−4% of MeOH, with water. The other reactants were the best available reagent grade and were used without further purification.

Instrumentation and Methods. GC analyses of liquid phase were performed using a "Tsvet-500" gas chromatograph equipped with a catharometer detector and a steel column (2 m × 3 mm) filled with Poropak-T [He, carrier gas; 110 °C (3 min) at 20°/min to 166 °C (11 min)]. The internal standard, ethanol, was added directly to an aliquot of the reaction mixture prior to GC measurements. Formaldehyde was also determined by a hydroxylamine method,[22] while formic acid was independently determined by titration with 0.05 M NaOH. The results of GC and titrimetric analyses coincided within 8−10%. Gas phase was analyzed using a "Tsvet-500" gas chromatograph equipped with a catharometer (He, carrier gas). Steel columns (2 m × 3 mm) filled with Poropak-T (98 °C) and Na-X (70 °C) were used for quantification of CO_2 and CO, respectively. ^{183}W and ^{17}O NMR spectra were recorded at 16.67 and 54.24 MHz, respectively, on an MSL-400 Brüker spectrometer. Chemical shifts, δ, were referenced to 1 M aqueous Na_2WO_4 and H_2O. Chemical shifts upfield from the reference are reported as negative. The error in measuring δ was in the range ±0.1 and ±3 ppm for ^{183}W and ^{17}O NMR, respectively. Infrared spectra were recorded as 0.5−1.0 wt % samples in KBr pellets on a Specord 75 IR or a Shimadzu FTIR-8300 spectrometer. Electronic absorption spectra were run on a Specord M40 spectrophotometer using 1- and 0.01-cm thermostated quartz cells. Cyclic voltammetric measurements were performed at 25 °C under argon using a three-electrode cell, a glassy-carbon working electrode, a platinum auxiliary electrode, and a Ag/AgCl reference electrode. The measurements were carried out in water containing 0.2 M NaCl as supporting electrolyte. The concentration of **1** was 1 mM.

Synthesis of $\{NaH_3[SiW_{11}CeO_{39}]\cdot 7H_2O\}_n$ ($\{NaH_3\mathbf{1}\}_n$) and other Ce−POMs. Synthesis of this POM was performed in a two-chamber electrodialyzer described earlier.[23,24] To 30 mL of an aqueous solution of 0.2 M $Na_8[SiW_{11}O_{39}]$ (^{183}W NMR (−δ in ppm, relative intensity in parentheses): 101.1(2), 117.2(2), 122.7(1), 129.6(2), 143.9(2), 177.8(2)) was added 2.604 g of $Ce(NO_3)_3\cdot 6H_2O$ resulting in a dark precipitate. This suspension was passed through the anodic chamber of the electrodialyzer. Turning on the current (density 0.1 A/cm^2) caused dissolution of the solid and a color change in the solution from dark to light yellow. During the first 0.5 h of dialysis, electrochemical oxidation of Ce(III) to Ce(IV) along with decationization of the solution (removing Na^+ from the anodic chamber) occurred. Further, current strength spontaneously decreased 5−10 times. The total time of the dialysis was 5 h. The analyte solution was concentrated at 30 °C at an air humidity of 40%, and the resulting solid was dried 1 h at 100 °C to give yellow plates of $\{NaH_3\mathbf{1}\}_n$. Yield 100%. Elemental analysis based on $Na_2H_6[(SiW_{11}CeO_{39})_2]\cdot 14H_2O$ (wt %, found/calcd): Na 0.73/0.78, Si 0.96/0.95, W 67.7/68.2, Ce 4.65/4.72. Weight loss upon calcination at 600 °C: 5.2/5.2. IR (KBr, cm^{-1}): 1005_{weak}, 965, 910, 780, 730_{weak}, 525. ^{183}W NMR of monomer **$NaH_3$1** as a result of dissociation of $\{NaH_3\mathbf{1}\}_n$ in solution (-δ in ppm, relative intensities in parentheses): 111.0(1), 116.0(2), 129.5(2), 151.4(2), 152(2), 178.5(2). ^{17}O NMR (δ in ppm, group assignments in parentheses): 24 (Si−O); 376, 393, 401, 407, 417 (W−O−W); 658 (W−O−Ce); 706, 713, 718, 730 (W═O). When the total time of the electrodialysis was only 0.5 h, a less acidic salt, $\{Na_{2.4}H_{1.6}[SiW_{11}CeO_{39}]\cdot 15H_2O\}_n$ ($\{\mathbf{Na_{2.4}H_{1.6}1}\}_n$), was formed. IR (KBr, cm^{-1}): 1010, 960, 900, 785, 730_{weak}, 515. ^{183}W NMR of **$Na_{2.4}H_{1.6}$1** (-δ in ppm, relative intensities in parentheses): 109.7(1), 115.8(2), 129.5(2), 150.6(2), 151.2(2), 177.6(2). Attempts to obtain a pure H^+ salt failed. $Cs_4H_4[(SiW_{11}CeO_{39})_2]\cdot 18H_2O$ (**$Cs_4H_4\mathbf{1}_2$**) was precipitated from the solution of $Na_{2.4}H_{1.6}[SiW_{11}CeO_{39}]$ by adding 24 mL of 1 M aqueous CsCl. The resulting yellow solid was recrystallized from water. IR (KBr, cm^{-1}): 1000, 965, 900, 790, 520. Elemental analysis based on $Cs_4H_4[(SiW_{11}CeO_{39})_2]\cdot 18H_2O$ (wt %, found/calcd): W 63.1/62.3, H 0.62/0.62, Si 0.83/0.87, Ce 4.32/4.32. X-ray quality yellow crystals of $Cs_8[(SiW_{11}Ce(OH_2)_3O_{39})_2]\cdot 24H_2O$ were grown by slow evaporation of H_2O (see crystallography details below). The Ce^{III} form of **NaH_3**1 was obtained by using bulk electrolysis of **$NaH_3$1** (5 mM) at E_{red} = 400 mV using 0.1 M NaCl as supporting electrolyte.

The dimer $Na_{10}(NH_4)_2[(SiW_{11}O_{39})_2Ce]\cdot 29H_2O$ was prepared by the procedure similar to that described in the literature.[25] IR (KBr, cm^{-1}): 1010_{weak}, 950, 890, 790, 730, 510. ^{183}W NMR (−δ): 108.5(2), 112.4(2), 113.0(2), 131.2(2), 134.9(2), 147.9(2), 148.8(2), 160.9(2), 162.2(2), 180.4(2), 201.3(2). $H_{10}[(PW_{11}O_{39})_2Ce]$,[23]

(10) Hill, C. L.; Prosser-McCartha, C. M. *Coord. Chem. Rev.* **1995**, *143*, 407−455.
(11) Neumann, R. *Prog. Inorg. Chem.* **1998**, *47*, 317−370.
(12) Mizuno, N.; Misono, M. *Chem. Rev.* **1998**, *98*, 199−218.
(13) Moffat, J. B. *Metal-Oxygen Clusters: The Surface and Catalytic Properties of Heteropoly Oxometalates*; Kluwer/Plenum: New York, 2001.
(14) Kozhevnikov, I. V. *Catalysis by Polyoxometalates*; Wiley: Chichester, 2002.
(15) *Polyoxometalate Molecular Science*; Borrás-Almenar, J. J., Coronado, E., Müller, A., Pope, M. T., Eds.; Kluwer: Dordrecht, 2003.
(16) Pope, M. T. Polyoxo Anions: Synthesis and Structure. In *Comprehensive Coordination Chemistry II*; Wedd, A. G., Ed.; Elsevier Science: New York, 2004; Vol. 4, pp 635−678.
(17) Hill, C. L. Polyoxometalates: Reactivity. In *Comprehensive Coordination Chemistry II*; Wedd, A. G., Ed.; Elsevier Science: New York, 2004; Vol. 4, pp 679−759.
(18) Gall, R. D.; Hill, C. L.; Walker, J. E. *J. Catal.* **1996**, *159*, 473−478.
(19) Kholdeeva, O. A.; Vanina, M. P.; Timofeeva, M. N.; Maksimovskaya, R. I.; Trubitsina, T. A.; Melgunov, M. S.; Burgina, E. B.; Mrowiec-Bialon, J.; Jarzebski, A. B.; Hill, C. L. *J. Catal.* **2004**, *226*, 363−371.
(20) Sadakane, M.; Dickman, M. H.; Pope, M. T. *Angew. Chem., Int. Ed.* **2000**, *39*, 2914−2916.
(21) Luo, Q. L.; Howell, R. C.; Bartis, J.; Dankova, M.; Horrocks, W. D.; Rheingold, A. L.; Francesconi, L. C. *Inorg. Chem.* **2002**, *41*, 6112−6117.
(22) Walker, J. F. *Formaldehyde*, 3rd ed.; Reinhold: New York, 1964.
(23) Maksimov, G. M.; Maksimovskaya, R. I.; Kozhevnikov, I. V. *Zh. Neorg. Khim.* **1992**, *37*, 2279−2286.
(24) Kulikova, O. M.; Maksimovskaya, R. I.; Kulikov, S. M.; Kozhevnikov, I. V. *Izv. Akad. Nauk SSSR, Ser. Khim.* **1991**, 1726−1732 (in Russian).
(25) Maksimova, L. G.; Denisova, T. A.; Yanchenko, M. Y.; Tutunnik, A. P.; Kristallov, L. V.; Efremova, N. N.; Vilisov, D. V. *Zh. Neorg. Khim.* **1997**, *42*, 1815−1820 (in Russian).

$Na_9[CeW_{10}O_{36}]$,[26] $Nd_2H_2[CeMo_{12}O_{42}]$,[27] $NaH_7[CeMo_{12}O_{42}]$,[28] $Ce_3H_3[(PMo_{11}O_{39})_2Ce]$,[29] and $Ce_3H_3[(PW_{11}O_{39})_2Ce]$[29] were prepared by literature procedures.

Catalytic Oxidations. Catalytic experiments were performed in 100-mL thermostated glass reactors filled with O_2 or air (1 atm). An aqueous solution (5 mL), containing formaldehyde and catalyst, was vigorously stirred at 20−40 °C. The formaldehyde and catalyst concentrations were varied in the ranges 0.117−0.960 and 0.002−0.012 M, respectively. Aliquots were taken from the liquid phase during the reaction course and analyzed by both GC and titrimetric methods. The initial rate method was employed to determine the reaction orders. Initial rates were determined as $d[CH_2O]/dt$ at $t = 0$. At least 2 measurements of reaction rate were obtained for every experiment. Separate determination of H_2O_2 and HCO_3H was performed as described previously.[30]

X-ray Crystallography. A suitable plate-shaped crystal of $Cs_8[(SiW_{11}Ce(OH_2)_3O_{39})_2]\cdot 24H_2O$ ($0.16 \times 0.15 \times 0.05$ mm^3) was coated with Paratone N oil, suspended on a small fiber loop, and placed in a cooled nitrogen stream at 173 K on a Bruker D8 SMART APEX CCD sealed tube diffractometer with graphite monochromated Mo Kα (0.71073 Å) radiation. A sphere of data was measured using a series of combinations of ϕ and ω scans with 10 s frame exposures and 0.3° frame widths. Data collection, indexing, and initial cell refinements were all handled using SMART software [*SMART*, version 5.55; Bruker AXS, Inc.: Madison, WI, 2000]. Frame integration and final cell refinements were carried out using SAINT software [*SAINT*, version 6.02; Bruker AXS, Inc.: Madison, WI, 1999]. The final cell parameters were determined from least-squares refinement. The SADABS program was used to carry out absorption corrections [Sheldrick, G. *SADABS*; University of Göttingen: Göttingen, Germany, 1996].

The structure was solved using direct methods and difference Fourier techniques [*SHELXTL*, version 5.10; Bruker AXS, Inc.: Madison, WI, 1997]. All the Ce, Cs, Si, and W atoms were refined with anisotropic thermal parameters. Nearly all of the oxygen atoms were also refined anisotropically, except O7, O16, O20, O28, O32, O34, O36, O37, and O9w. Bond valence sum (BVS) calculations were done on Ce1 (3.94) and O7 (2.01), the μ-oxo bridging atom. Constants for the BVS calculations were accepted values.[31] The final R1 scattering factors and anomalous dispersion corrections were taken from the *International Tables for X-ray Crystallography*.[32] Structure solution and refinement were performed by using SHELXTL, V5.10 software [*SHELXTL*, version 5.10; Bruker AXS, Inc.: Madison, WI, 1997]. See Table S2 in SI for the crystal data and structure refinement parameters.

Results and Discussion

Synthesis and Characterization of $NaH_3[SiW_{11}CeO_{39}]$. The existence of $SiW_{11}CeO_{39}^{4-}$ was inferred previously from solution cyclic voltammetry studies;[33] however, in contrast to the phosphorus analogue, $PW_{11}CeO_{39}^{3-}$,[23] it had never been isolated. In this work, the Ce(IV)-substituted heteropolytungstate **$NaH_3$1** (**$(\{NaH_3\mathbf{1}\}_n$** in the solid-state) was prepared using the electrodialysis method.[23,24] The purity of **$NaH_3$1** was confirmed by elemental analysis (see Experimental Section), IR, and cyclic voltammetry. The IR spectrum of solid **1** displays a fingerprint region that is characteristic of monosubstituted Keggin POMs (Figure 1). The cyclic voltammogram of **$NaH_3$1** (see the SI, Figure S1) is close to that published in the literature.[33] The UV−vis spectrum of **$NaH_3$1** indicates that cerium is in the form of Ce(IV) (pale yellow) rather than Ce(III) (orange)[20] (Figure S2). Potentiometric titration with methanolic TBAOH confirmed the presence of three acid protons in the molecule of **$NaH_3$1** (Figure S3). A sharp breakpoint was observed upon addition of 3 equiv of TBAOH to **1**.

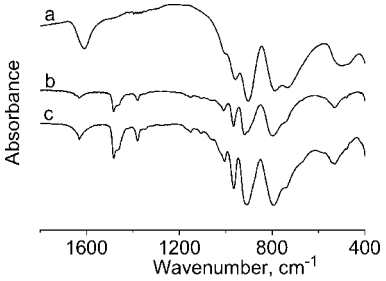

Figure 1. IR spectra of $\mathbf{1}_n$ in KBr (0.5−1 wt %): (a) $\{NaH_3[SiW_{11}CeO_{39}]\}_n$; (b) TBA salt of $\mathbf{1}_n$ precipitated before the reaction; and (c) TBA salt of $\mathbf{1}_n$ precipitated after the reaction (reaction conditions: $[CH_2O] = 0.467$ M, $[\mathbf{NaH_3 1}] = 0.003$ M, 1 atm air, 40 °C, 5 h).

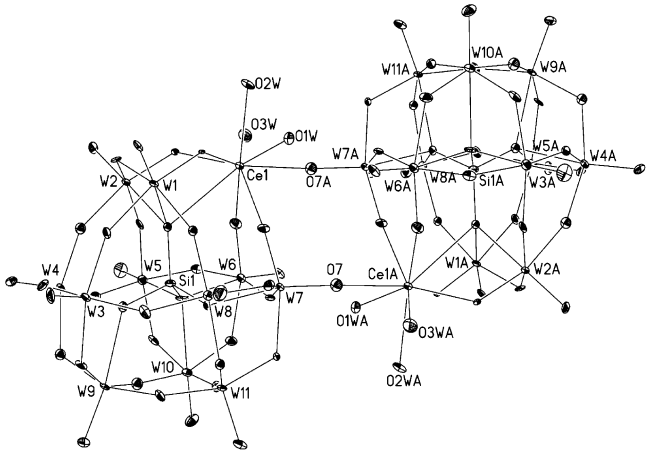

Figure 2. Thermal ellipsoid plot (50% probability) of $\mathbf{1_2}$ (R1 = 5.79%).

The X-ray structure of the cesium salt revealed the dimeric structure of **$Cs_8\mathbf{1}_2$** (Figure 2). In this dimer, each Ce(IV) is bound to a terminal W═O moiety of the other Keggin unit (oxidation states confirmed by bond valence sum (BVS) in the SI). This type of binding and equilibrium is precedented for Ce-containing and other lanthanide-containing POMs.[20,21] Three coordination sites of the Ce(IV) ions are occupied by water molecules, which can be, in principle, replaced by reactant molecules. Both IR and cyclic voltammetry studies of **$Cs_8\mathbf{1}_2$** and **$NaH_3$1** confirmed the identity of polyanions in these two salts.

Prior to catalytic studies, ^{183}W NMR was used to assess the structure of the POM in solution (Figure 3). At

(26) Peacock, R. D.; Weakley, T. J. R. *J. Chem. Soc. A* **1971**, 1836−1839.
(27) Samokhvalova, E. P.; Molchanov, V. N.; Tatyanina, I. V.; Torchenkova, E. A. *Koord. Khim.* **1990**, *16*, 1277−1282 (in Russian).
(28) Baidala, P.; Torchenkova, E. A.; Spitsin, V. I. *Dokl. Acad. Nauk USSR* **1971**, *196*, 1344−1345 (in Russian).
(29) Maksimov, G. M. *Zh. Neorg. Khim.* **2000**, *45*, 1451−1452 (in Russian).
(30) Greenspan, F. P.; Makkellar, D. G. *Anal. Chem.* **1948**, *20*, 1061−1063.
(31) (a) Roulhac, P. T.; Palenik, G. J. *Inorg. Chem.* **2003**, *42*, 118−121. (b) Brown, I. D.; Altermatt, D. *Acta Crystallogr., Sect. B* **1985**, *41*, 244−247.
(32) *International Tables for X-ray Crystallography*; Kynoch Academic Publishers: Dordrecht, Netherlands, 1992; Vol. C.
(33) Haraguchi, N.; Okaue, Y.; Isobe, T.; Matsuda, Y. *Inorg. Chem.* **1994**, *33*, 1015−1020.

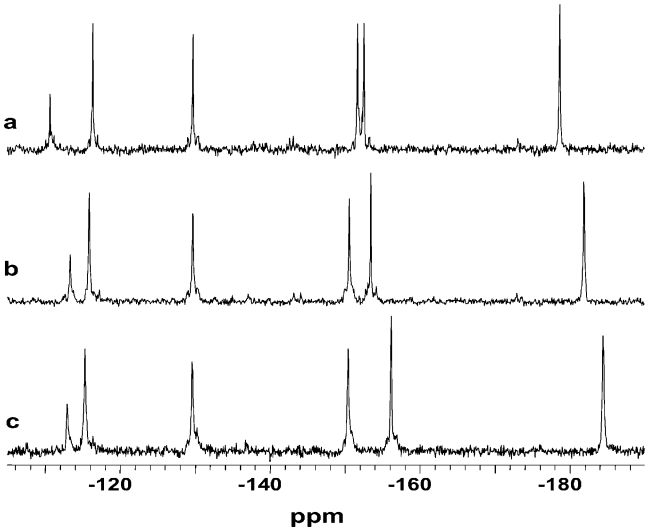

Figure 3. ^{183}W NMR spectra of **NaH$_3$1** in H_2O at 20 °C at (a) 0.3 M, (b) 0.6 M, and (c) ~0.8 M.

Table 1. Aerobic Oxidation of Formaldehyde in Water in the Presence of Ce-Containing Compounds[a]

catalyst	CH_2O conversion (%)	yield of HCOOH[b] (%)	TON[c]
without catalyst	0	0	–[d]
$H_4SiW_{12}O_{40}$	0	0	
$K_8SiW_{11}O_{39}$	0	0	
$NaH_3SiW_{11}CeO_{39}$ (**NaH$_3$1**)	15	14	3.4
$Na_{2.4}H_{1.6}SiW_{11}CeO_{39}$	2	–	–
$Cs_2H_2SiW_{11}CeO_{39}$	3	2	0.7
$Na_3PW_{11}CeO_{39}$	0	0	–
$H_{10}[(PW_{11}O_{39})_2Ce]$	1	0	–
$Na_{10}(NH_4)_2[(SiW_{11}O_{39})_2Ce]$	4	4	0.9
$Ce(NO_3)_3$	0	0	–
$(NH_4)_2Ce(NO_3)_6$	0	0	–
$Ce(SO_4)_2$[e]	9	9	2.0

[a] Reaction conditions: $[CH_2O] = 0.117$ M, [catalyst] = 5.2 mM, 1 atm of air, 5 mL of H_2O, 40 °C, 5 h. [b] GC yield based on initial CH_2O. [c] TON = turnover numbers = (moles of CH_2O consumed/moles of catalyst). [d] Not determined. [e] $[H_2SO_4] = 0.125$ M.

concentrations 0.1−0.8 M in H_2O, it is clear that no 11-line spectrum, demanded by $\mathbf{1_2}$ (C_i symmetry), is present. Only the 6-line spectrum of the dissociated monomer (C_s symmetry) is observed. Thus, at the lower concentrations required by the catalysis (see below), the complex almost surely exists as monomer **1**. However, the reactivity of some dimer present under catalytic conditions cannot be unequivocally ruled out.

Aerobic Formaldehyde Oxidation. In the presence of catalytic amounts of **NaH$_3$1**, aqueous solutions of formaldehyde simply exposed to the air are oxidized to formic acid with high selectivity (Table 1), and the reaction proceeds by the stoichiometry in eq 1. Formic acid was stable under the reaction conditions; no products of its oxidation were found in independent experiments even at 60 °C. Only traces (<0.5%) of CO and CO_2 are present by GC in the reactions performed at 20−60 °C, and no methylformate is detected (limit ~1%). The titrimetric method described in the literature[30] indicates that both H_2O_2 and HCO_3H are intermediates in these reactions (Figure 4). There is no detectable reaction in the absence of **1**. Interestingly, dimeric Ce−POMs, $Na_{10}(NH_4)_2[(SiW_{11}O_{39})_2Ce]$, and $H_{10}[(PW_{11}O_{39})_2Ce]$ show very low activity in the formaldehyde oxidation (Table 1), most likely as a consequence of coordinate saturation and nonlability of the Ce centers in these POMs. It is noteworthy that $Na_{2.4}H_{1.6}SiW_{11}CeO_{39}$ and $Na_3PW_{11}CeO_{39}$ were practically inactive compared to **NaH$_3$1** (Table 1), indicating that the number of protons in the Ce−POM is a crucial factor in catalytic activity.

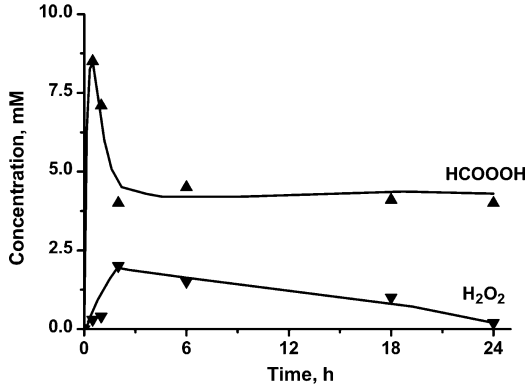

Figure 4. H_2O_2 and HCO_3H concentrations versus time in the oxidation of CH_2O (0.175 M) by air (1 atm) in the presence of **NaH$_3$1** (6 mM) in H_2O at 40 °C.

Table 2. Aerobic Oxidation of CH_2O in Water in the Presence of NaH_31[a]

[**1**] × 10^3 (M)	$[CH_2O]$ (M)	CH_2O conversion (%)	yield of HCOOH[b] (%)	TON[c]
12.4	0.117	9	8	0.8
12.4[d]	0.117	10	9	0.9
6.2	0.117	20	20	3.8
6.2[d]	0.117	21	20	4.0
3.1	0.117	15	14	5.7
1.6	0.117	11	10	8.0
3.1	0.233	18	17	13.5
3.1	0.467	20	19	30.1
12.4	0.467	25	23	9.4

[a] Reaction conditions: 1 atm of air, 40 °C, 5 h. [b] GC yield based on initial CH_2O. [c] Turnover numbers (TON) = moles of CH_2O consumed/moles of catalyst. [d] 1 atm of O_2 was used instead of air.

The stoichiometric oxidation of formaldehyde with Ce(IV) in aqueous acid solutions was reported in the early 1970s.[34−36] We have found that $Ce(SO_4)_2$ showed some catalytic activity in the aerobic formaldehyde oxidation; however, reaction requires a significant excess of H_2SO_4 (Table 1). In the absence of acid, $Ce(SO_4)_2$ is insoluble in water, and CH_2O conversion is very low. The higher activity of **NaH$_3$1** derives in part from a synergy between a redox active metal and protons.

Optimization of the reaction conditions led to a system that afforded 30 turnovers of **NaH$_3$1** after 5 h (Table 2). The IR spectra of $\mathbf{1_2}$, precipitated as its n-Bu_4N^+ salt before and after reaction (30 turnovers), show no change whatsoever, implying that the system (**1** and $\mathbf{1_2}$) is stable under turnover conditions (Figure 1b,c). Despite the stability of the catalyst, the reaction stops after ca. 25% conversion of CH_2O. Although it was determined that formic acid inhibits the reaction (Figure S4), no evidence for POM−formate association is observed spectroscopically.

(34) Sakhla, P. S.; Mehrotra, R. N. *J. Inorg. Nucl. Chem.* **1972**, *34*, 3781−3788; *Indian J. Chem.* **1972**, *10*, 1081−1084.
(35) Wadhawan, A. K. *Indian J. Chem.* **1973**, *11*, 567−570.
(36) Emanuel, N. M.; Denisov E. T.; Maizus, Z. K. *Chain Reactions of Hydrocarbon Oxidation in Liquid Phase*; Nauka: Moscow, 1965.

Four lines of evidence are consistent, not surprisingly, with radical chain character in the mechanism.[36−40] First, the reaction is retarded by small amounts of radical chain scavengers, such as 2,6-di-*tert*-butyl-4-methylphenol (ionol) and hydroquinone (Figures 5 and S5). Some nonradical chain processes can be inhibited by these compounds (false positives). Also, some authentic radical chain processes are unaffected by addition of conventional quantities of some scavengers (false negatives) when the rate constant for biomolecular radical scavenging is small relative to those for propagation and sometimes others in the reaction. Nonetheless, the degree of inhibition we observe at the scavenger concentrations used constitutes fairly strong evidence for the presence of at least one radical chain. Second, the rate is not effected by the O_2 pressure (Table 2). Autoxidation, including aldehyde autoxidation, is independent of O_2 pressure when the chains are reasonably long, i.e., when the two propagation steps, e.g., eqs 4 and 5, dominate product formation.[41] This follows, because for any reasonable chain length, eq 6 holds, and at the typical concentrations of substrate and O_2 pressures used in our reactions (and generally at O_2 pressures > 0.1 atm), $[RCO^{\bullet}] \ll [RCO_3^{\bullet}]$ and the rate is independent of O_2 pressure. Liquid-phase autoxidation rates are typically independent of O_2 concentration for O_2 pressures of 0.1 atm or more (as in our case).[39]

$$\text{initiation: } X^{\bullet} + RCHO \rightarrow RCO^{\bullet} + HX \quad (3)$$

$$\text{propagation: } RCO^{\bullet} + O_2 \rightarrow RCO_3^{\bullet} \quad (4)$$

$$RCO_3^{\bullet} + RCHO \rightarrow RCO_3H + RCO^{\bullet} \quad (5)$$

$$k_4[O_2][RCO^{\bullet}] \sim k_5[RCO_3^{\bullet}][RCHO] \quad (6)$$

Third, the rate is first order in formaldehyde and goes through a maximum with increasing concentration of both heteropolyanion at constant pH and **$NaH_3$1** (Figures 6 and S6, respectively). Such bell-shaped (or parabolic) dependences of rate on catalyst/initiator concentration are frequently seen in homolytic chain processes but in very few other classes of reactions. Such kinetic behavior is as indicative of radical-chain character as any other single feature. These dependences derive primarily from a superposition of initiation and inhibition processes both involving the catalyst/initiator. Hiatt and co-workers, Black, and other groups have provided experimental data that clarify the multiple component processes extant in initiation−inhibition phenomena seen in radical chain oxidations. The roles of catalyst/initiator properties, catalyst concentration, and the nature of the medium in this chemistry are now reasonably well understood.[42,43] Fourth, the rate does not exhibit an Arrhenius temperature dependence (Figure S7). This indicates that multiple rate-limiting steps are operable over the evaluated temperature range. This is a common feature for processes whose overall kinetic order and the key processes in the mechanism change with reaction conditions including the percent conversion. This latter factor leads to the next complication in many metal-catalyzed O_2-based condensed-phase oxidations, namely that formation of the ultimate product (formic acid in our case) is largely controlled by processes after or in addition to the initiation, propagation, and termination steps dominant at the outset of autoxidation (eqs 3−5 and radical−radical combination). These include, but are not limited to, the primary Haber−Weiss homolytic peroxide decomposition processes and Baeyer−Villiger oxidation of reactant aldehyde by the formal autoxidation product, the peracid. (Note that autoxidation followed by Haber−Weiss chemistry is sometimes referred to as "radical-chain oxidations with chain branching".)[44]

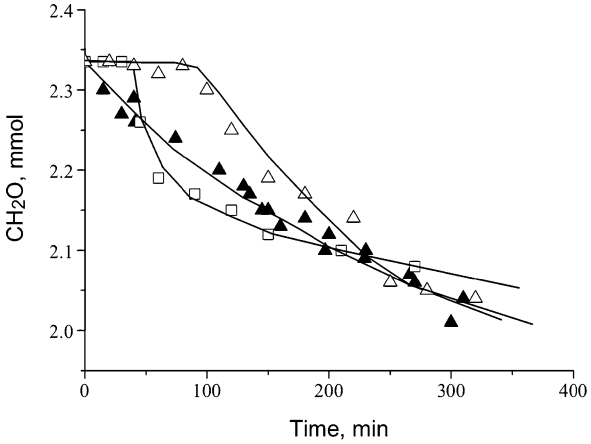

Figure 5. CH_2O consumption in the presence of 0.023 mmol of **1** (H_2O 5 mL; 1 atm of air; 40 °C): (▲) without additives; (□) 0.0085 mmol of ionol was added at the beginning of the reaction, and (△) 0.017 mmol of ionol was added at the beginning of the reaction.

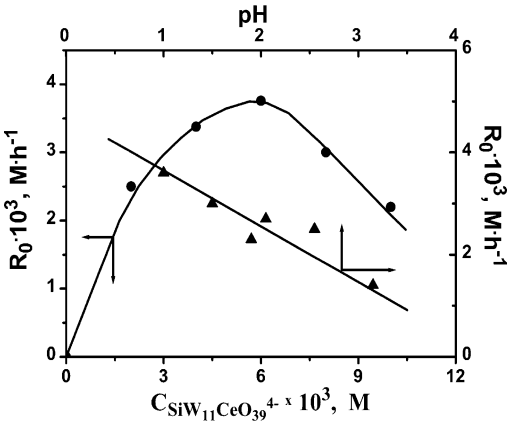

Figure 6. Initial rates of the CH_2O oxidation (●) versus concentration of **$NaH_3$1** at pH = 1.85 and (▲) versus pH at [**$NaH_3$1**] = 6 mM ([CH_2O] = 0.175 M).

(37) Sheldon, R. A.; Kochi, J. K. *Metal-Catalyzed Oxidations of Organic Compounds*; Academic Press: New York, 1981.
(38) Vardanyan, I. A.; Nalbandyan, A. B. *Russ. Chem. Rev.* **1985**, *54*, 903−922.
(39) Kholdeeva, O. A.; Grigoriev, V. A.; Maksimov, G. M.; Fedotov, M. A.; Golovin, A. V.; Zamaraev, K. I. *J. Mol. Catal. A*: *Chem.* **1996**, *114*, 123−130.
(40) Kholdeeva, O. A.; Khavrutskii,I. V.; Romannikov, V. N.; Tkachev, A. V.; Zamaraev, K. I. *Stud. Surf. Sci. Catal.* **1997**, *110*, 947−955.
(41) Denisov, E. T.; Mitskevich, N. I.; Agabekov, V. E. *Liquid-Phase Oxidation of Oxygen-Containing Compounds*; Consultants Press: New York, 1977; Chapter 1.
(42) Hiatt, R.; Irwin, D. C.; Gould, C. W. *J. Org. Chem*. **1968**, *33*, 1430−1435.
(43) Black, J. F. *J. Am. Chem. Soc.* **1978**, *100*, 527−535.

The Haber−Weiss chain in our chemistry, eqs 7 and 8, is not only known to be important in aldehyde autoxidation, but also specific to our work, Ce salts have been documented to participate in these processes. In addition, the literature study examined Ce acetylacetonates[42] which have Ce in a very similar coordination environment to the Ce in our catalyst **1** (both the acetylacetonates and the lacunary polytungstate ligand have exclusively oxygen ligands with all oxygens having a low effective negative charge). In our oxidations, the electronic absorption spectrum stays that of Ce(IV) throughout the reaction (the spectra of the authentic Ce(III) and Ce(IV) complexes are quite distinct and given in the Supporting Information). This argues for the facility of Ce(III) reoxidation to the Ce(IV) form (eq 8). The potentials and rates predict that the Ce(IV) form would be dominant under steady-state conditions (e.g., eq 7 is rate limiting in the Haber−Weiss breakdown chain). The rate of oxidation of the Ce^{III}−POM by O_2 is negligible under the reaction conditions which is not surprising given $Ce^{IV/III}$ and O_2/H_2O reduction potentials. (The potential for **$NaH_3$1** is 0.609 V versus Ag/AgCl; Figure S1.)

$$RCO_3H + Ce^{IV} \rightarrow RCO_2^{\bullet} + H^+ + Ce^{III} \quad (7)$$

$$RCO_3H + Ce^{III} \rightarrow RCO_2^{-} + OH^{\bullet} + Ce^{IV} \quad (8)$$

Two points address the H^+ dependence of the catalyzed reaction. First, as we mentioned above, the more protonated forms of the initial solid $\mathbf{1}_2$ are more reactive (Table 1), and second, the reaction rate decreases linearly with pH (Figure 6). This indicates that protonation of CH_2O (and likely proton-induced dehydration, eq 9) and/or protonation of the POM is likely involved. The former process, acid-assisted dehydration of the predominant formal form of formaldehyde, followed by oxidation of the resulting carbocation, was suggested earlier in the stoichiometric oxidation of CH_2O by $Ce(SO_4)_2/H_2SO_4$.[45] One argument for oxidation of the carbocation (eq 10) (versus oxidation of formal) is that the effective concentration of the carbocation proximal to the POM will be higher than that of the neutral formal because of carbocation−POM electrostatic attraction. On the basis of quantitative dynamic ion pairing studies of POMs during oxidation,[46−48] it is very likely that any carbocation−POM interaction is transient and that the ions are freely diffusing in the solvent used in these catalytic studies (H_2O). The argument against carbocation oxidation is that it is a weaker reducing agent than the formal. In reality, both formal and carbocation oxidation may be operable. This cannot be distinguished by the kinetic data. Clearly, protonation of the POM, **1**, would increase the rate and driving force for the oxidation (the protonated POM is a better oxidant), regardless of whether the reactant is the carbocation, eq 10, or the more nucleophilic and stronger reductant, the formal.

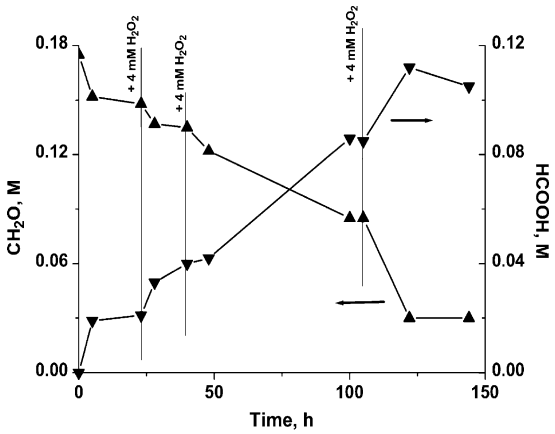

Figure 7. Oxidation of CH_2O (0.175 M) by air (1 atm) in the presence of **$NaH_3$1** (6 mM) in H_2O at 40 °C.

$$CH_2(OH)_2 + H^+ \rightarrow H_2COH^+ + H_2O \quad (9)$$

$$H_2COH^+ + [H_xSiW_{11}Ce^{IV}O_{39}]^{(4-x)-} \rightarrow HCO^{\bullet} + [H_xSiW_{11}Ce^{III}O_{39}]^{(5-x)-} + H^+ \quad (10)$$

Literature studies have implicated the $HCO^{\bullet}$ radical which reacts with O_2 to give $HO_2^{\bullet}$, $HCO_3^{\bullet}$, and $OH^{\bullet}$ radicals, that participate in chain propagation.[38,49] All the data presented here together with literature studies indicate we likely have multiple initiating species, all the well-established processes in both aldehyde autoxidation and Haber−Weiss peroxide radical-chain decomposition processes, Baeyer−Villiger reaction of formaldehyde reactant by intermediate peroxyformate and inhibition by formate product. Goldstein, Meyerstein, and Czapski in their authoritative review based on years of study of Haber−Weiss and related Fenton-like metal-catalyzed reactions have concluded that identifying all the oxidizing intermediates in such reactions is simply impossible in many instances.[50] This certainly appears to be a defensible stance. We feel that the superposition of this complexity in the aerobic oxidation of formaldehyde by **1** with the complex dependence of the rate of this chemistry on the concentration of **1** makes writing an insightful rate law for the overall process a questionable if not futile exercise.

After the concentration of H_2O_2 becomes negligible, the reaction stops. This suggested that addition of small portions of H_2O_2 during the course of the reaction might increase the CH_2O conversion. Indeed, a stepwise addition of small amounts (4 mM) of H_2O_2 (a total of 0.016 mol of H_2O_2 per 0.15 mol of CH_2O consumed) increases the CH_2O conversions up to 85%, producing a 66% yield of HCOOH (25 turnovers) after 122 h (Figure 7).

(44) *Autoxidation and antioxidants*; Lundberg, W. O., Ed.; Interscience: New York, 1961.
(45) Husain, M. *J. Inorg. Nucl. Chem.* **1977**, *39*, 2249−2252.
(46) Grigoriev, V. A.; Hill, C. L.; Weinstock, I. A. *J. Am. Chem. Soc.* **2000**, *122*, 3544−3545.
(47) Grigoriev, V.; Hill, C. L.; Weinstock, I. A. In *Oxidative Delignification Chemistry. Fundamental and Catalysis*; Argyropoulos, D. S., Ed.; ACS Symposium Series; American Chemical Society: Washington, DC, 2001; Chapter 18, pp 297−312.
(48) Grigoriev, V. A.; Cheng, D.; Hill, C. L.; Weinstock, I. A. *J. Am. Chem. Soc.* **2001**, *123*, 5292−5307.
(49) Maslov, S. A.; Bumberg, A. A. *Russ. Chem. Rev.* **1976**, *65*, 303−328.
(50) Goldstein, S.; Meyerstein, D.; Czapski, G. *Free Radical Biol. Med.* **1993**, *15*, 435−445.

Conclusions. The Ce-containing complex $[SiW_{11}CeO_{39}]^{4-}$, **1**, has been prepared using an electrodialysis method and thoroughly characterized in both the solid state and in solution. This POM catalyzes the aerobic oxidation of formaldehyde to formic acid under very mild (including ambient) conditions. The reaction rate exhibits a clear H^+ dependence and nonlinear dependences on catalyst/initiator concentration and temperature. The complex mechanism involves both autoxidation and Haber−Weiss radical-chain processes (both H_2O_2 and HCO_3H intermediates are quantifiable), inhibition by formate product, and a change in the dominant and rate-limiting steps with a change in reaction conditions, including the percent conversion. Optimization of the reaction conditions led to a system that afforded 30 turnovers of **$NaH_3$1** after 5 h. The catalyst is stable under turnover conditions and exists as monomer **1** in solution and as dimer $\mathbf{1_2}$ in the solid-state. Conversions of CH_2O up to 85% with a 66% yield of HCOOH can be achieved in the presence of small amounts of H_2O_2. Systematic optimization and mechanistic studies are in progress.

Acknowledgment. CRDF (Grant RC1-2371-NO-02) funded the research. We thank Yurii Geletii for fruitful discussions.

Supporting Information Available: List of POMs and POM-based combinations tested in the oxidation of CH_2O and crystallographic (CIF), spectroscopic, and kinetic data. This material is available free of charge via the Internet at http://pubs.acs.org.

IC049109O